The Analysis of a Ferriteless Rectangular Coupler With Reactive Assistive shielding Coils For EV Wireless Charging

Shuo Wang
National Engineering Lab of Electrical Vehicle & Collaborative Innovation Center for Electric Vehicle
Beijing Institute of Technology
Beijing, China
Shuo.Wang@bit.edu.cn

Zhenpo Wang
National Engineering Lab of Electrical Vehicle & Collaborative Innovation Center for Electric Vehicle
Beijing Institute of Technology
Beijing, China
Wangzhenpo@bit.edu.cn

Junjun Deng
National Engineering Lab of Electrical Vehicle & Collaborative Innovation Center for Electric Vehicle
Beijing Institute of Technology
Beijing, China
Dengjunjun@bit.edu.cn

Youguang Guo
Faculty of Engineering and IT
University of Technology, Sydney
Sydney, Australia
Youguang.Guo@uts.edu.au

David G. Dorrell
School of Engineering
University of Kwazulu-Natal
Durban, South Africa
dorrelld@ukzn.ac.za

***Abstract*—Autonomous driving technology has made significant progress in recent decades. For fully autonomous driving of an electric vehicle, the recharging process should be possible without a manually fixed connection. Wireless charging technology is a promising solution for electric vehicle recharging automation. The wireless transformer/coupler is the key component in electric vehicle wireless charging. The maximum power transfer capability and efficiency are limited by the coupler. To reach the required power level, efficiency and electromagnetic exposure to surrounding area, the coupler should be analyzed. In this paper, a coupler with assistive coils is presented and analyzed. The assistive coils perform as reactive shielding coils as well as flux concentrating coils. Finite element simulation and circuit simulation results are shown.**

Keywords—Wireless Charging, Electric Vehicle, Reactive Shielding, Flux Concentrating

I. INTRODUCTION

With the development of electric vehicle related technology, the driving range of electric vehicles has reached 400 km and is expected to increasing in the coming years. The driving range is not the major concern for many EV consumers, however, it is the "charging time trauma" which is still an obstacle. Electric vehicles still often require an entire night to recharge with a regular charger and maybe an hour or more at a commercial fast recharging station for a fill-up. Wireless charging has the potential to create more recharging windows for EVs. These have gained a lot of attention in recent years. At the same time, development of autonomous driving has made notable progress in the past decade. Self-parking technology has been developed on many commercial vehicles. For the future level 5 autonomous driving, the fully-autonomous system is expected to perform equally to a human driver in every driving scenario [1]. Therefore, the charging should be autonomous as well and wireless charging technology is a competitive choice for autonomous vehicle charging.

The wireless charging technology which is most widely employed is inductive charging [2-12]. The general structure of a inducive wireless charging system is shown in Fig. 1. It has a high frequency (HF) power source, a wireless transformer, and a rectifier. Wireless charging has three key areas: 1) wireless transformer design; 2) compensation circuit configuration and power electronics design; and 3) system control.

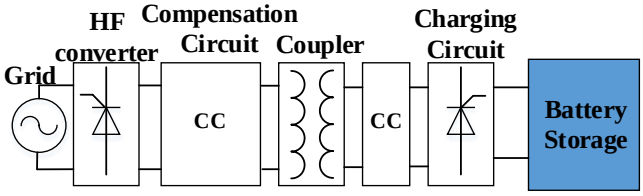

Fig. 1. General structure for wireless charging system

The output frequency of the high frequency inverter ranges from 10 kHz to several tens of MHz [2]. For many high power applications, such as EV wireless charging, maximum efficiency is sought in order to reduce the recharging cost. A power source with a small impedance is preferred so that most of power can be transferred to the load. With the development of SiC and GaN devices, inverters switching at greater than 100 kHz, which have low switching losses, are available for wireless charging applications.

The coupler is the key component to transfer the power across the airgap. The high frequency current in the primary side generates alternating magnetic field which induces voltages in the secondary side winding. With the compensation circuit connected to the secondary side winding output, the power is transferred to the batteries via the rectifier. The receiving pad is carried on board with vehicle; therefore, there are more restriction on its size and weight. Comparing to the receiving pad, the ground pad should to be strong enough to

support a passenger car weight and it has less limitation on the size and the weight.

The size of the primary coupler can be larger than the secondary side, and by employing a larger primary coupler, the rated power and efficiency can be higher. Larger primary pads create higher electromagnetic exposure to surrounding areas, which is restricted by the wireless charging standards such as SAE J2954 and IEC61980. Also, for practical parking situations, it is hard to achieve perfect alignment between the primary pad and the secondary pad. The flux leakage causes eddy current loss in the vehicle chassis. The misalignment may cause reduction of power transfer capability and efficiency.

Even when pads are perfectly aligned, with different types of secondary pad design, the leakage flux still induces eddy current loss which heats up the chassis and lowers the system efficiency. For example, if the primary side pad is a DD pad, and the secondary pad is a circular pad, the centers of the primary and secondary pads may not be on the same vertical line of the ground plane. If the secondary pad is embedded in the chassis, part of the metal chassis would be over the top of a primary D coil. This part of steel vehicle chassis is then exposed to the flux from primary side without ferrite and aluminium plate as shielding. The unmatched pads also give a higher leakage in regions 2 and 3. Therefore, the coupler shielding is used to reduce the electromagnetic exposure to surrounding areas and it could play an important role in achieving interoperability between different types of coupler.

There are passive shielding [13], reactive shielding [14] and active shielding methods [15]. The simplest passive shielding method is to use metal plate to absorb the electromagnetic energy and keep the magnetic field in surrounding areas. The changing magnetic field causes eddy current losses in the shielding plate and therefore adding metal plate shielding would reduce the system efficiency. Another type of shielding is reactive shielding which uses the mitigating effectiveness of a coil. The mitigating effectiveness relies on the generation coil currents whose magnetic field partially counteracts that generated by the coupler. The shielding magnetic field not only depends on the induced current magnitude, but also on the geometry and location of the shielding coils. Active shielding uses a power source to generated current in the shielding coils; there is a degree phase difference between the primary side current and shielding coil current. The shielding coil-generated magnetic field will mitigate the coupler magnetic field. The current in the active shielding coils can be adjust by controlling the power source magnitude. The active shielding requires extra power sources which increases the system cost.

Both active and reactive coil shielding adds extra coils into the coupler, which forms a multi-coil coupler structure. For EV wireless charging, two-coil and four-coil structures are widely used and have been studied by many researchers. For a multi-coil coupler, with extra coils added to primary coil, the magnetic field distribution is reshaped. In [16] and [17], coaxial coils are added into primary side coupler, which enhanced the transfer efficiency and the double boost effect. In [18], an extra coil was series-connected in the reverse direction to reduce the leakage of the primary coil.

For reactive shielding, the current in the shielding coils creates a magnetic field that is opposite to the leakage magnetic field, which reduces the RMS value of the EM exposure. Passive shielding also induces current into coil windings and causes copper losses in the winding. In [19], the shielding coils were designed to be decoupled with secondary side coil. Therefore, there is no flux linkage between the shielding coil and secondary coil, and the shielding coil is not involved in the power transfer process. In this paper, an inductive wireless charging coupler with two primary side assistive coils are studied. The assistive coils work as shielding coils and they lead to a flux concentrating effect which enhances the coupler power transfer capability.

II. INDUCTIVE POWER TRANSFER SYSTEM

A wireless transformer has a primary coupler powered by high frequency power source and a secondary side which is connected to the vehicle battery charger. Generally, the primary coupler is isolated from secondary coupler by an airgap. The electrical power will be transferred from the primary coupler to secondary coupler across the airgap via a magnetic link. Many wireless transformer geometries have been proposed, including a two-coil structure and a multi-coil structure. The two-coil structure has one coil on the primary side and one coil on the secondary side. Each coil can be formed by one or more windings connected in a series or parallel combination. For the multi-coil structure, there is an extra resonant coil or compensation coil in either or both primary or secondary sides. The extra coils are short circuit or connected to a compensation capacitor circuit. Both the two winding and multi winding structures are single phase applications. For single phase application, there can be multiple winding structures, but they can be treated as a combination of two or multi-winding systems. There is limited research on multi-phase structures. This is probably due to the complexities of a wireless transformer design and the control of the charging system.

A. Two Winding Structure

The two coil system is widely used in inductive charging applications. Fig. 2 shows the equivalent circuit, where L_1 and L_2 are the inductances of the primary and secondary windings; C_1 and C_2 are the compensation capacitors, and series-series (SS) capacitor compensation is used here; R_1 and R_2 are the resistances of the windings and capacitors, and R_{load} is the load for the wireless charging system, respectively.

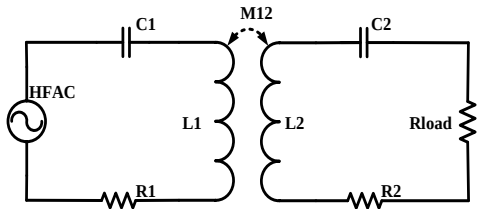

Fig. 2. General structure for series-series compensation.

The voltage equations can be written as

$$U = Z_1 I_1 + j\omega M_{12} I_2 \quad \text{and} \quad 0 = j\omega M_{21} I_1 + Z_2 I_2 \tag{1}$$

$$Z_1 = R_1 + j\omega L_1 - \frac{j}{\omega C_1} \text{ and } Z_2 = R_2 + R_{load} + j\omega L_2 - \frac{j}{\omega C_2} \tag{2}$$

Assuming that the inductance is fully compensated by the capacitor at the HFAC frequency $\omega L_1 = 1/\omega C_1$, and mutual inductance $M = M_{12} = M_{21}$, then

$$U = \left[R_1 + \frac{(\omega M)^2}{R_2 + R_{load}} \right] I_1 \tag{3}$$

$$j\omega M Y_{11} U_1 = \left(R_{eq} + R_2 + R_{load} \right) I_2 \tag{4}$$

$$R_{eq} = R_1 + \frac{(\omega M)^2}{R_2 + R_{load}} \tag{5}$$

Therefore, the ratio between I_1 and I_2 is

$$\frac{|I_1|}{|I_2|} = \frac{\left(R_{eq} + R_2 + R_{load} \right)}{\omega M R_1 R_{eq}} = \frac{\left(R_{eq} + R_2 + R_{load} \right)}{kQR_1 R_{eq}} \tag{6}$$

The efficiency of the two coils system is

$$\eta = \frac{I_2^2 R_{load}}{\left(I_2^2 \left(R_{load} + R_2 \right) + I_1^2 R_1 \right)} \tag{7}$$

B. Three Coil structure

It is possible so use either three of four coils. A four-coil system was reported in [11]. Impedance matching between the input and output is applied to acquire the maximum power output in low power applications, which often have a system efficiency lower than 50 %. In [12], the maximum efficiency principle is employed for a four-coil EV wireless charging system. In [16], a coaxial three-coil structure is employed and is further developed into coaxial four coil structure with two enhance coils in the primary side. The general structure of three winding system is shown in Fig. 3.

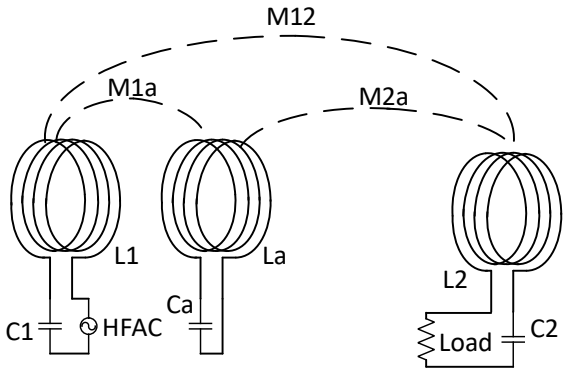

Fig. 3. General structure for three coil system.

The system is driven by a high frequency power source. The circuit equation matrix for a three coil system is

$$\begin{bmatrix} U_0 \\ 0 \\ 0 \end{bmatrix} = \begin{bmatrix} Z_1 & j\omega M_{1a} & j\omega M_{12} \\ j\omega M_{1a} & Z_a & j\omega M_{2a} \\ j\omega M_{21} & j\omega M_{2a} & Z_2 \end{bmatrix} \begin{bmatrix} I_1 \\ I_a \\ I_3 \end{bmatrix} \tag{8}$$

$$\text{where} \quad \begin{aligned} Z_{1,a} &= R_{w1,wa} + j\omega L_{1,a} - 1/j\omega C_{1,a} \\ Z_2 &= R_{w2} + j\omega L_2 - 1/j\omega C_2 + R_{load} \end{aligned} \tag{9}$$

and M is the mutual inductance between two coils. The power output to the load is

$$P_{out} = |I_2|^2 R_{load} \tag{10}$$

The efficiency of the three coil system is

$$\eta = \frac{P_{out}}{P_{out} + P_{loss}} = \frac{|I_2|^2 R_{load}}{|I_2|^2 R_{load} + \sum_{i=1,a,2} |I_i|^2 R_i} \tag{11}$$

III. Reactive Shielding Analysis

The active shielding could generate required EM field to cancel the leakage flux; however, it requires at least one extra high frequency power source which is more expensive compared to the passive shielding. Several passive shielding topologies with extra windings are studied in [14-16].

In [18], the passive shielding windings are added outside the primary winding. The passive winding is short circuit with a capacitor. When the coupler is excited, the EMF will induce a voltage across the winding. To obtain maximum magnetic field cancelation, the phase of the cancelling magnetic field is perfectly opposite to the leakage magnetic field. To achieve the phase different from primary coil and secondary coil current, the assistive coil circuit should work in the inductive or capacitive region. Therefore, the assistive circuit resonance frequency should be different from both the primary and secondary side resonance frequencies.

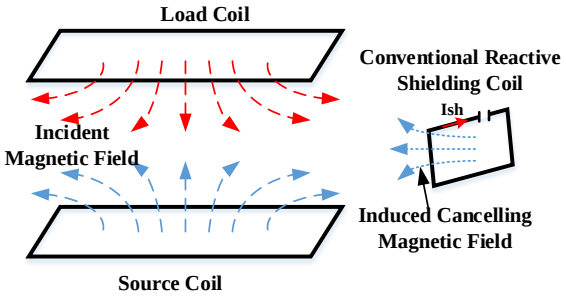

Fig. 4. Principle for reactive shielding

The induced current in the assistive coil can be written as

$$i_a = \frac{V_a}{Z_{eq}} == -\frac{j\omega M_{1a} i_1 + j\omega M_{2a} i_2}{\left(j\omega L_a - \frac{j}{\omega C_a} \right) + R_a} \tag{12}$$

When the secondary and the assistive coils are decoupled, $M_{2a} = 0$,

$$i_a = -\frac{i_1 M_{1a}}{\left(j\omega L_a - \frac{j}{\omega C_a} \right) + R_a} \tag{13}$$

When $j\omega L_a > \frac{j}{\omega C_a}$, the assistive coil circuit is in the inductive region, assume the $j\omega L_{eq} \gg R_a$,

$$i_a = \frac{V_a}{Z_{eq}} = -\frac{j\omega M_{1a} i_1}{j\omega L_{eq}} \tag{14}$$

$$B_a = \frac{\mu_0}{2r_a} N_a i_a = \frac{\mu_0}{2r_a} N_a \frac{V_a}{Z_{eq}} = -\frac{\mu_0}{2r_a} N_a \frac{i_1 M_{1a}}{L_{eq}} \tag{15}$$

$$B_1 = \frac{\mu_0}{2r_1} N_1 i_1 = -K B_a \tag{16}$$

The phase of the magnetic field generated by the assistive coil in the closed area of the coil is opposite to the primary coil in inductive region. When the mutual inductance between L_a and L_2 is 0, there is no flux linkage between them. The assistive coils only act as passive shielding.

IV. Coupler Analysis

A. Coupler FEA Simulation

Since the wireless transformer is a loosely coupled transformer, the leakage flux is high. To reduce this, the magnetic field needs to be modified so that the flux linkage between two sides is increased and the leakage is reduced. A coupler with assistive coils is shown in Fig. 5.

Fig. 4 shows a 3D view, while Fig. 5(b) shows the top view of the primary coupler and Fig. 5(a) shows a side view. The Y direction sides of the major coil has two small assistive coils, which is used to as a shielding coil. The two assistive coils are connected in series or parallel, forming an assistive winding, which makes it a three-coils system. When the major coils have clockwise directional current, the assistive windings has anti-clockwise directional current when the assumption in section III is met. The assistive coil current creates opposite EMF at inside the assistive coil area and outside the major coil. At the same time, the EMF in the area between major coil and two assistive windings are enhanced.

In this paper, SS connected compensation is analyzed. The transformer is simulated in ANSYS Maxwell 3D. The parameters for the transformer are shown in Table I. The frequency of the system is set to 85 kHz; hence, Litz-Wire is used to reduce eddy current loss.

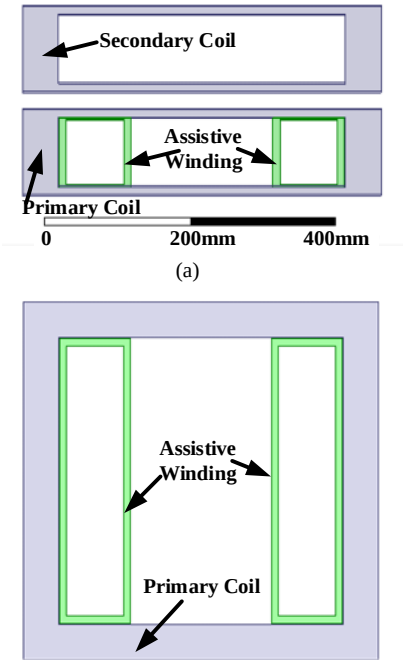

Fig. 5. Coupler Geometry a) Side View of Coupler b) Top View of Primary Coupler

Table I. Coupler Size Parameter

Coil	Size (mm)	Width(mm)
Primary(Outer)	500 × 500	50
Assistive Winding(Outer)	400 × 100	10
Secondary Winding(Outer)	500 × 500	50
Airgap	150	N/A

FEA simulation results for the coupler winding self-inductance and mutual inductance without misalignment are shown in Table II. When there is a misalignment between the primary side and the secondary side, the coupling between primary coil and assistive coil does not change as the relative positions are still the same. The mutual inductance M_{12} between the primary and secondary coils, and M_{a2} between the assistive and secondary coils, varies with X and Y direction misalignment. M_{12} versus X and Y direction misalignment is shown in Fig. 6. M_{a2} versus X and Y direction misalignment is shown in Fig. 7. The decrease in M_{12} with the increase in misalignment distance can be noted, and M_{a2} has the same trend. However, the decrease in M_{a2} is slower in the Y direction compared to the X direction.

Table II. Self-inductance and Mutual inductance between Coils

$L1$	94.08 uH
$L2$	94.23 uH
La	123.40 uH
$Ma1$	33.336 uH
$Ma2$	5.69 uH
$M12$	15.90 uH

B. Circuit Analysis

For wireless charging system with a three-coil coupler, the assistive coil also requires compensation to achieve high system efficiency. To evaluate the performance of the coupler, the assistive coil compensation capacitance is evaluated with the circuit model in Section II.*B*.

The coupler winding parameters are as shown in Table I. Series-series compensation is used for the primary and secondary coils, and for both, the resonance frequency is set to the power source frequency. All winding resistances are set to 0.1 Ω.

The system efficiency versus C_a is shown in the Fig. 8. The assistive circuit resonance frequency is close to the power source frequency of 85 kHz when the capacitance is 28.4 nF. The system efficiency is low when the assistive circuit resonance frequency is close to power source frequency, and the system efficiency reaches 0 when the assistive compensation capacitance is 29.9 nF.

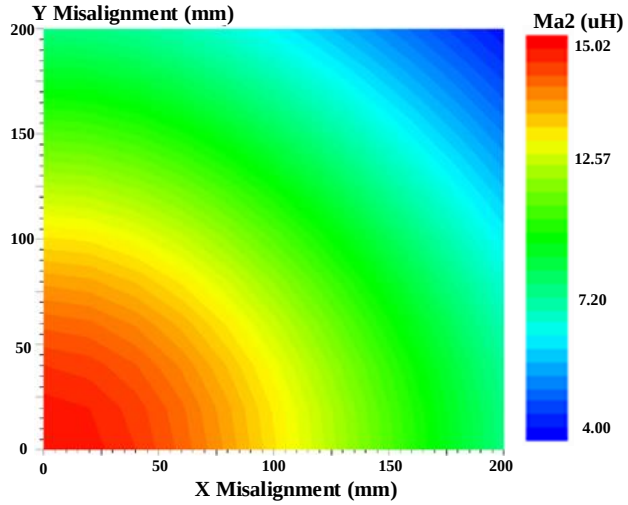

Fig. 6 M12 versus X and Y direction Misalignment

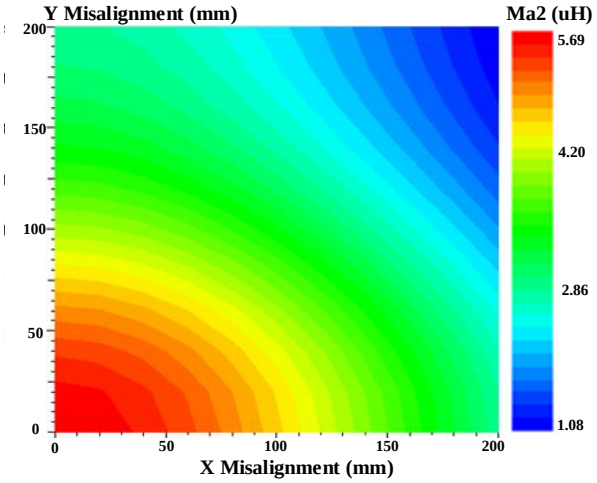

Fig. 7 *Ma*2 versus X and Y Direction Misalignment

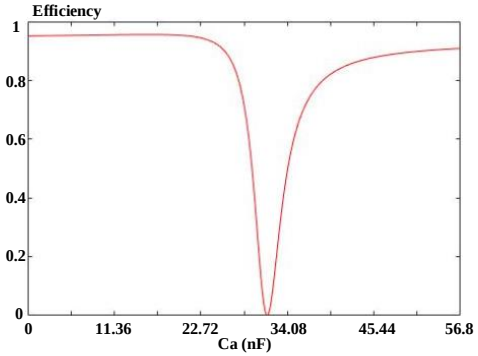

Fig. 8 System efficiency versus Ca Equations

C. *Magnetic Field Analysis*

To get the magnetic field distribution of a WPT system with a three-coil coupler, the magnitude and phase of the current in each coil are required. The circuit simulation model is shown as Fig. 9(a), and the two-coil model is shown in Fig. 9(b). The coupler parameters are as in Table II, and the compensation parameters are as in Section IV.*B*. The current waveforms are shown in the Fig. 10. Fig. 10(a) shows the waveforms of the three-coil system and Fig. 10(b) shows the waveforms of the two coil system. The red curve is the primary coil current and blue curve is the assistive coil current and the green curve is the secondary coil current. I_1 and I_a have a phase difference close to 180 degrees.

The RMS value of the currents are shown in Table III. Both the three coil and two coil systems have a output power of 7.59 kW, while three-coil system efficiency is 93.99 %, the two coil system has a lower efficiency of 92.01 %. The three-coil system also has a lower input current I_1 compared to the two-coil system input current. This shows that for the two types of coupler, with same power ratio, the three-coil coupler could use thinner Litz-wire for the primary coil. The thinner Litz-wire has less strands and is cheaper than thick wires.

TABLE III CIRCUIT SIMULATION RESULT

Three Coil	Two Coils
I_1 = 45.39 A rms	I_1 = 63.7A rms
I_a = 16.4 A rms	N/A
I_2 = 50.3 A rms	I_2 = 50.3A
Efficiency = 93.99 %	Efficiency = 92.01 %
P_{out} = 7.59 kW	P_{out} = 7.59 kW

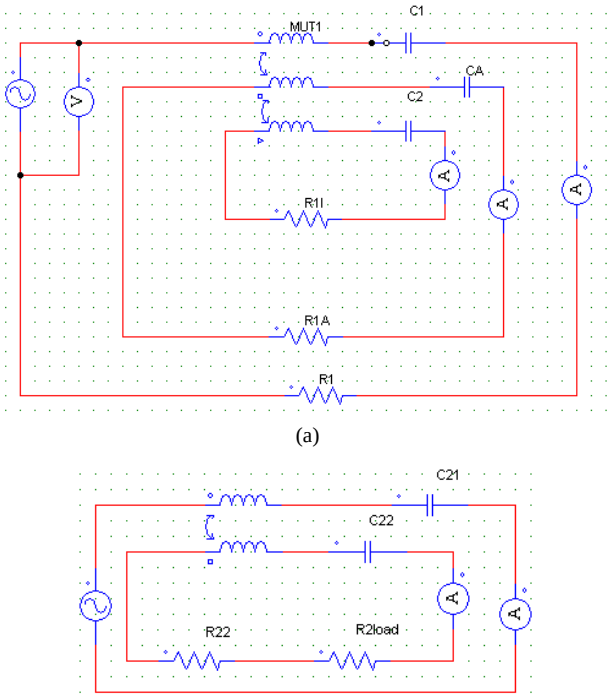

(a)

(b)

Fig. 9 Circuit Simulation Model (a) Three Coil Model (b) Two Coil Model

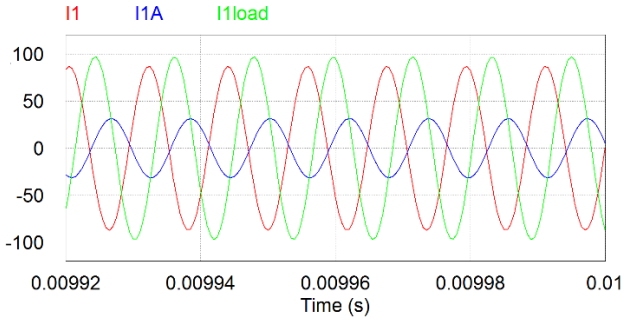

(a)

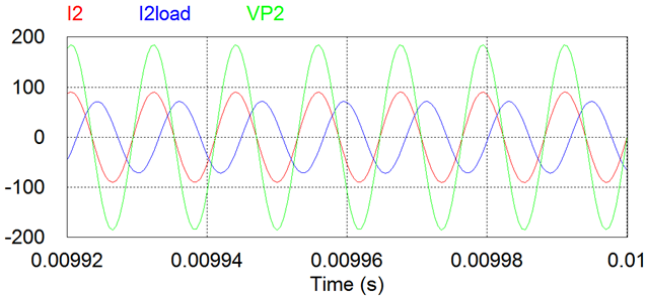

(b)

Fig. 10 Circuit Simulation Model (a) Three Coil Model (b) Two Coil Model

The results in Table III is used for coupler FEA simulation. The flux density on the surface, which is 150 mm above primary coupler, is shown in Fig. 11. Fig. 11(a) shows that of the three coil coupler and Fig. 11(b) shows that of the two coil system. The flux density contour of the two coil system has a similar shape to the primary coil, while the flux density contour of the three coil system is similar to retangular. It shows that the assistive coil reshaped the magnetic field, and the coupler with an assistive coil could enhance the system efficiency.

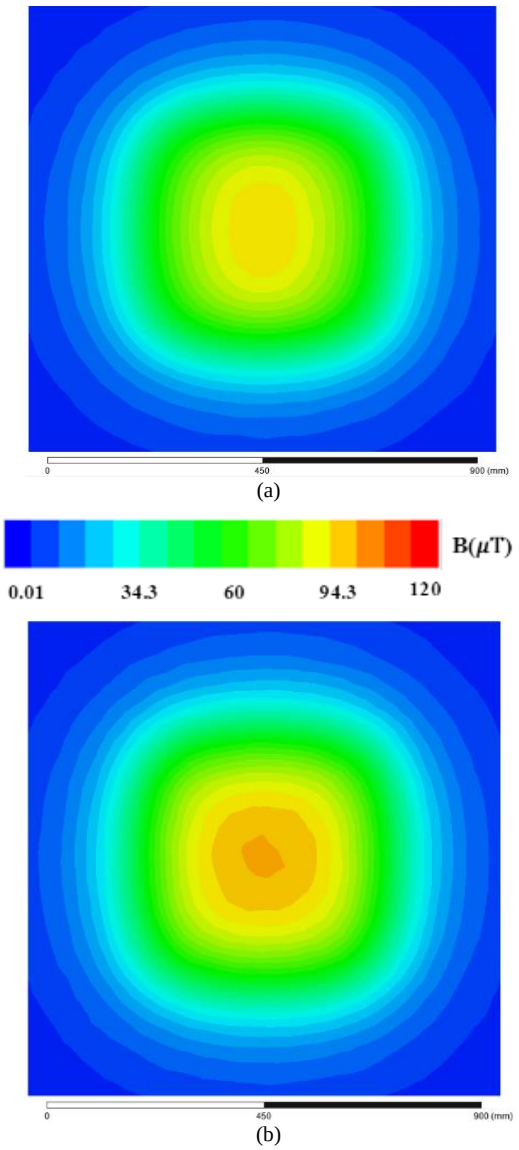

Fig. 11 Flux density at the secondary coil surface (a) Three Coil (b) Two Coils.

I. CONCLUSION

The analysis of a wireless charging system with a three-coil coupler was presented. The three-coil coupler consists of an assistive coil which acts as a shielding coil and has a flux concentrating effect for the primary and secondary linkage flux. The flux concentrating effect of the shielding coil has been shown from the simulation results. The compensation capacitance for the reactive shielding circuit has been analyzed. The circuit has been simulated and the flux density has been obtained from FEA simulation. The FEA simulation shows that the magnetic field is reshaped by the assistive coil. And for the same power output, the system efficiency is enhanced with less current in the primary coil. The angular misalignment will be discussed in future work.

ACKNOWLEDGMENT

This work was supported in part by the National Key R&D Program under Grant 2018YFB0105400 and in part by NSFC under Grant 51707010.

REFERENCES

[1] "Taxonomy and Definitions for Terms Related to Driving Automation Systems for On-Road Motor Vehicles," ed: SAE International, 2016.

[2] S. Y. R. Hui, W. Zhong, and C. K. Lee, "A Critical Review of Recent Progress in Mid-Range Wireless Power Transfer," *IEEE Trans on Power Electronics, vol. 29, pp. 4500-4511, 2014*.

[3] W. Chwei-Sen, O. H. Stielau, and G. A. Covic, "Design considerations for a contactless electric vehicle battery charger," *IEEE Trans. on Ind.l Electron.*, vol. 52, pp. 1308-1314, 2005.

[4] M. Budhia, J. T. Boys, G. A. Covic, and H. Chang-Yu, ""Development of a single-sided flux magnetic coupler for electric vehicle IPT charging systems," *IEEE Trans. on Ind. Electron.*, vol. 60, pp. 318-328, 2013.

[5] S. Wang and D. G. Dorrell, "Review of wireless charging coupler for electric vehicles," *IEEE IECON Conference*, Vienna, Nov 2013.

[6] F. Musavi, M. Edington, and W. Eberle, ""Wireless power transfer: A survey of EV battery charging technologies," *IEEE ECCE*, 2012, pp. 1804-1810.

[7] G. A. Covic, L. G. Kissin, D. Kacprzak, N. Clausen, and H. Hao, "A bipolar primary pad topology for EV stationary charging and highway power by inductive coupling," *IEEE ECCE*, Sep. 2011, pp. 1832–1838.

[8] Y. H. Kim, S. Y. Kang, S. Cheon, M. L. Lee, J. M. Lee, and T. Zyung, "Optimization of wireless power transmission through resonant coupling," *SPEEDAM*, 2010, pp. 1069–1073.

[9] S. Cheon, Y. H. Kim, S. Y. Kang, M. L. Lee, J. M. Lee, and T. Zyung, "Circuit-model-based analysis of a wireless energy-transfer system via coupled magnetic resonances*," IEEE Trans. Ind. Electron*., vol. 58, no. 7, pp. 2906–2914, Jul. 2011.

[10] P. Si, A. P. Hu, J. W. Hsu, M. Chiang, Y. Wang, S. Malpas, and D. Budgett, "Wireless power supply for implantable biomedical device based on primary input voltage regulation," *2nd IEEE Conf. Ind. Electron. Appl*., May 2007, pp. 235–239.

[11] A. Kurs, A. Karalis, R. Moffatt, J. D. Joannopoulos, P. Fisher, and M. Soljacic, "Wireless power transfer via strongly coupled magnetic resonances," *Science*, vol. 317, no. 5834, pp. 83–86, Jul. 2007

[12] Q. Zhu, L. Wang, and C. Liao, "Compensate Capacitor Optimization for Kilowatt-Level Magnetically Resonant Wireless Charging System," *IEEE Transactions on Industrial Electronics*, vol. 61, pp. 6758-6768, 2014.

[13] P. Cruz, C. Izquierdo, and M. Burgos, "Optimum passive shields for mitigation of power lines magnetic field," *IEEE Transactions on Power Delivery*, vol. 18, pp. 1357-1362, 2003.

[14] M. Hwansoo, K. Sungkyu, P. Hyun Ho, and A. Seungyoung, "Design of a Resonant Reactive Shield With Double Coils and a Phase Shifter for Wireless Charging of Electric Vehicles," *IEEE Transactions on Magnetics*, vol. 51, pp. 1-4, 2015.

[15] S. Kim, H.-H. Park, J. Kim, J. Kim, and S. Ahn, "Design and Analysis of a Resonant Reactive Shield for a Wireless Power Electric Vehicle," *IEEE Transactions on Microwave Theory and Techniques*, vol. 62, pp. 1057-1066, 2014.

[16] S. Moon, B. Kim, S. Cho, C. Ahn, and G. Moon, "Analysis and Design of a Wireless Power Transfer System With an Intermediate Coil for High Efficiency," *IEEE Transactions on Industrial Electronics*, vol. 61, pp. 5861-5870, 2014.

[17] S. Moon and G. Moon, "Wireless Power Transfer System With an Asymmetric Four-Coil Resonator for Electric Vehicle Battery Chargers," *IEEE Transactions on Power Electronics*, vol. 31, pp. 6844-6854, 2016.

[18] A. Tejeda, C. Carretero, J. T. Boys, and G. A. Covic, "Ferrite-Less Circular Pad With Controlled Flux Cancelation for EV Wireless Charging," *IEEE Transactions on Power Electronics*, vol. 32, pp. 8349-8359, 2017.

[19] Q. Zhu, Y. Zhang, Y. Guo, C. Liao, L. Wang, and L. Wang, "Null-Coupled Electromagnetic Field Canceling Coil for Wireless Power Transfer System," IEEE Transactions on Transportation Electrification, vol. 3, pp. 464-473, 2017.